ACS APPLIED MATERIALS & INTERFACES

Research Article

www.acsami.org

Patterned Free-Standing Conductive Nanofilms for Ultraconformable Circuits and Smart Interfaces

Francesco Greco,*[,†] Alessandra Zucca,[†,‡] Silvia Taccola,[†] Barbara Mazzolai,[†] and Virgilio Mattoli[†]

[†]Center for MicroBioRobotics @SSSA, Istituto Italiano di Tecnologia, Viale Rinaldo Piaggio 34, 56025 Pontedera, Italy

[‡]The Biorobotics Institute, Scuola Superiore Sant'Anna, Viale Rinaldo Piaggio 34, 56025 Pontedera, Italy

Supporting Information

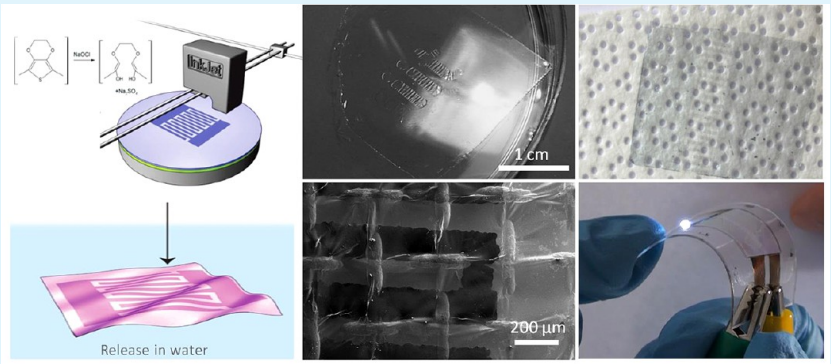

ABSTRACT: A process is presented for the fabrication of patterned ultrathin free-standing conductive nanofilms based on an all-polymer bilayer structure composed of poly(3,4-ethylenedioxythiophene)/poly(styrene sulfonate) and poly(lactic acid) (PEDOT:PSS/PLA). Based on the strategy recently introduced by our group for producing large area free-standing nanofilms of conductive polymers with ultrahigh conformability, here an inkjet subtractive patterning technique was used, with localized overoxidation of PEDOT:PSS that caused the local irreversible loss of electrical conductivity. Different pattern geometries (e.g., interdigitated electrodes with various spacing, etc.) were tested for validating the proposed process. The fabrication of individually addressable microelectrodes and simple circuits on nanofilm having thickness ∼250 nm has been demonstrated. Using this strategy, mechanically robust, conformable ultrathin polymer films could be produced that can be released in water as free-standing nanofilms and/or collected on surfaces with arbitrary shapes, topography and compliance, including human skin. The patterned bilayer nanofilms were characterized as regards their morphology, thickness, topography, conductivity, and electrochemical behavior. In addition, the electrochemical switching of surface properties has been evaluated by means of contact angle measurements. These novel conductive materials can find use as ultrathin, conformable electronic devices and in many bioelectrical applications. Moreover, by exploiting the electrochemical properties of conducting polymers, they can act as responsive smart biointerfaces and in the field of conformable bioelectronics, for example, as electrodes on tissues or smart conductive substrates for cell culturing and stimulation.

KEYWORDS: *conducting polymer, conformable electronics, nanofilm, patterning, inkjet, PEDOT:PSS*

1. INTRODUCTION

1.1. Stretchable and Conformable Electronics. Research on flexible, stretchable, and conformable electronics has grown in the last two decades, due to the huge number of applications in which such developments could be used, from consumer electronics to energy, robotics, or also biomedicine.[1,2] The challenge is to transfer the consolidated semiconductor technologies (integrated circuits fabrication, mainly restricted to planar, brittle and rigid systems, as wafers) to soft and rubbery substrates. Crucial to this aim is the selection of materials: while retaining the same functional properties for their use in electronic devices, they must possess the suitable mechanical properties allowing for deformation (stretching, compression, bending, twisting) or for conformability to surfaces with arbitrary roughness and complex topography. As regards stretchable electrodes, different composite structures have been developed in recent years based on conductive layers deposited over elastomeric substrates, both by employing micro-nanostructured inorganic materials, such as microcracked or wrinkled gold on poly(dimethylsiloxane) (PDMS)[3,4] or stretchable Au electrodes made of multilayers of Au nanosheets on rubber substrates,[5] or by using organic conductors and semiconductors, as in the case of buckled poly(3,4-ethylenedioxythiophene)/poly(styrene sulfonate) (PEDOT:PSS) over PDMS.[6,7] Besides approaches based on developing novel materials with tailored mechanical properties (i.e., allowing for

Received: June 3, 2013
Accepted: August 26, 2013
Published: August 26, 2013

   dx.doi.org/10.1021/am402142c | ACS Appl. Mater. Interfaces 2013, 5, 9461−9469

stretching), other researchers faced the challenge by employing new structural forms of well-known and established materials.[8] The latter case is exemplary represented by serpentine metal structures and silicon devices embedded in silicones by the Rogers group[9−11] that permitted development of epidermal electronic systems. These systems are characterized by conformal contact and adhesion to skin, and they incorporate several electronic devices (sensors, transistors, LED, photodetectors, RF inductors) and power supply (solar cells, wireless coils).[12] Further developments comprised the use of conformable ultrathin metal electrode arrays on silk fibroin to be used as bioresorbable biointerfaces.[13] Recently, highly stretchable electric circuits have been prepared from a composite material made of silver nanoparticles and elastomeric fibers, starting from a nanoparticle precursor that was absorbed in electrospun poly(styrene-*block*-butadiene-*block*-styrene) (SBS) rubber fibers.[14]

1.2. Conducting Polymers and Organic Electronics. Organic conductors and semiconductors have been as well applied in the development of microfabricated conformable bioelectronic devices such as microelectrode arrays to be used as in vivo recording systems and biointerfaces.[15,16] As regards organic electronic materials, in general their flexibility, tunability of physical properties, stimuli-responsiveness, combined with the capability of processing over large areas with low-cost fabrication techniques, make them attractive materials for the fabrication of stretchable/flexible/conformable devices. Among other CPs, PEDOT:PSS in particular has found use in a variety of applications in organic electronics.[17] Indeed its high work function, which can be further optimized by various means, such as incorporation of secondary doping agents, makes it suitable as a hole transport layer in organic or polymer light-emitting diodes (OLEDs or PLEDs).[18−20]

Moreover, due to some unique features such as good cytocompatibility, optical transparency, and, above all, the ability to transport ions as well as electrons, there is a growing interest in the application of conducting polymers (CPs) at the interface with life sciences. This is the emerging field of "organic bioelectronics".[21,22] Based on the electron-ion transducer behavior of CPs, several devices have been developed with potential applications in tissue engineering and biosensing, such as organic electronic ion pumps, capable of controlled and localized delivery of biomolecules to cells or tissues,[23,24] or organic electrochemical transistors.[25] As in other "smart materials", many properties of CPs change reversibly upon oxidation/reduction; smart surfaces and biointerfaces made of polypyrrole (PPy), PEDOT or polythiophenes with switchable properties allow for electrochemical switching/control of wettability, cell-adhesion,[26−28] protein binding and conformation.[29−31] While the cited contributions mostly relies on the use of thin CPs films as an active coating over other bulk (bio)substrates, CPs themselves could allow to combine tailored mechanical properties for stretchability/conformability with the desired smart behavior in order to fabricate devices that operate both in dry (electronic conduction) or wet (ionic conduction) environment.

1.3. Conducting Polymer Nanofilms. Recently, we presented some methods for producing ultrathin conformable PEDOT:PSS free-standing nanofilms that can be released in water from the temporary substrate onto which they were prepared, maintaining their integrity and function.[32,33] Depending on the specific method that was used, nanofilms consisted of a single-layer of conductive polymer or embedded multiple layers (such as polyelectrolytes or other polymers). Due to their nanoscale thickness (≈30−300 nm) and large surface area (several cm^2), these nanofilms were able to float in water as free-standing membranes, to conform to rough or complex surfaces when collected over solid substrates, providing a simple and effective way to provide a soft conductive "skin", or also to stay as suspended conductive nanomembranes when collected over frames or holes.

Here we present a process for the fabrication of free-standing nanofilms with patterned conductivity, based on an all-polymer bilayer structure with total thickness of ∼250 nm composed by poly(3,4-ethylenedioxythiophene)/poly(styrene sulfonate) and poly(lactic acid) (PEDOT:PSS/PLA), with the latter polymer acting as a mechanical support layer for maintaining continuity and robustness. By using a subtractive patterning technique based on inkjet deactivation/etching of the conducting polymer, different pattern geometries (individually addressable microelectrodes and simple circuits) could be fabricated on board of the nanofilms that retained the desired ultraconformability. The patterned nanofilms were characterized as regards their morphology, thickness, topography, and conductivity; some simple demonstrators were built assessing the use of nanofilms as ultrathin, conformable electronic devices operating in air that could find use in many (bio)electrical applications. Moreover, by taking advantage of the change in wettability of the surface upon redox activation of PEDOT:PSS, we could appreciate the selective switching of the surface. Based on these findings, patterned nanofilms could find applications as responsive smart biointerfaces and in the field of conformable bioelectronics, for example, as soft electrodes on tissues, neural interfaces, smart conductive substrates for cell culturing and stimulation or as part of biohybrid devices.

2. EXPERIMENTAL SECTION

2.1. Materials. Silicon wafers used as substrates for nanofilm fabrication were cut in squares of approximately 2.5 cm length, rinsed with deionized water, and dried. Poly(dimethylsiloxane) (PDMS, Sylgard 184 silicone elastomer base and curing agent) was purchased by Dow Corning Corp. A PEDOT/PSS aqueous dispersion, Clevios PH 1000 (1:2.5 PEDOT:PSS ratio; H.C. Starck GmbH, Leverkusen, Germany) has been employed after filtration (Minisart, average pore size 1.20 μm, Sartorius). Poly(lactic acid) (PLA, average M_w = 60 kDa) was purchased from Sigma-Aldrich and used as received. Poly(vinylalcohol) (PVA; average molecular weight M_w = 30 kDa) was purchased by Sigma-Aldrich and used as received. *n*-Hexane (electronic use grade, 97%, Acros Organics), chloroform (≥99.5%, Sigma-Aldrich), dimethyl sulfoxide (DMSO, ACS Reagent, 99.9%, Sigma-Aldrich), sodium hypochlorite solution (purum, ∼10%, Sigma-Aldrich), and Triton X-100 (laboratory grade, Sigma Aldrich) were used without any further purification.

2.2. Fabrication of Bilayer PEDOT:PSS/PLA Nanofilms. Bilayer PEDOT:PSS/PLA nanofilms were prepared by properly modifying a similar procedure already reported in the case of single layer free-standing PEDOT:PSS nanofilms, as reported in Figure 1.[32] PDMS (10:1 ratio of base elastomer to curing agent) was diluted with *n*-hexane by 10% w/w. The diluted PDMS solution was spin-coated onto Si substrates for 150 s at a speed of 6000 rpm (Figure 1b) and then cured at T = 95 °C for 60 min in an oven, in order to obtain a thin elastomer film of final thickness $t \approx$ 800−1000 nm. Plasma activation of the PDMS surface (60 s, 5 W, Colibrì plasma system, Gambetti, Italy) was then carried out in order to temporarily improve its wettability. The PEDOT/PSS aqueous dispersion (Clevios PH 1000) was mixed with DMSO (5 wt %) for 8 h at RT with the aid of a magnetic stirrer, and then it was spin-coated at spin rate s = 2500 rpm for 60 s (Figure 1c). Samples at different thicknesses were also prepared by changing the spin rate in the range s = 1000−5000 rpm, in

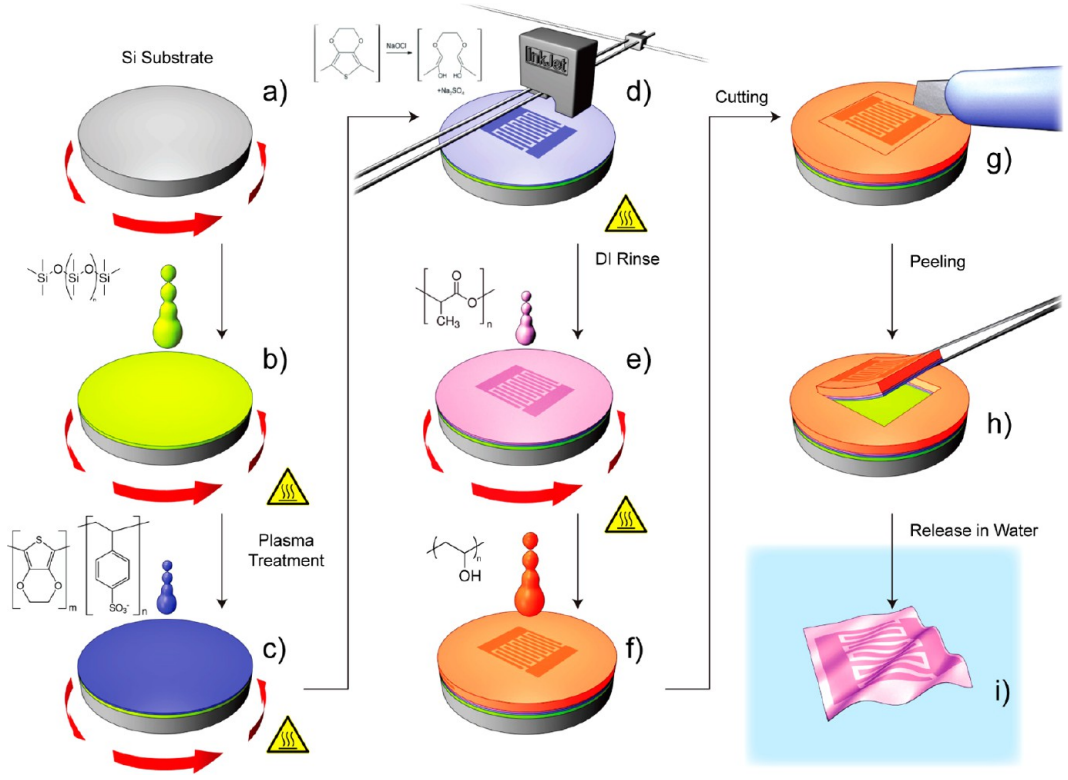

Figure 1. Scheme of bilayer PEDOT:PSS/PLA nanofilms fabrication, patterning, and release in water.

order to characterize thickness and conductivity. Then, samples underwent a thermal treatment (1 h; T = 170 °C). A PLA solution (chloroform, c = 20 mg/mL) was spin-coated on the PEDOT:PSS at s = 4000 rpm for 40 s and dried on a hot plate at T = 80 °C for 1 min (Figure 1e).

A water-soluble supporting layer of PVA was deposited on top of the previous layers, by drop casting a PVA solution in DI water (c = 100 mg/mL) that was allowed to dry overnight at RT (Figure 1f). After 8 h (needed for hydrophobic recovery of PDMS, see section 3.1), the sample edges were cut with a razor blade (Figure 1g) and the three-layered film (PEDOT:PSS/PLA/PVA) was peeled off from the PDMS substrate with the aid of tweezers (Figure 1h). By dissolving the supporting PVA layer in DI water, the free-standing bilayer PEDOT:PSS/PLA nanofilm was finally obtained (Figure 1i).

2.3. Nanofilms Patterning. Patterned bilayer nanofilms were obtained by including a step of inkjet patterning of PEDOT:PSS in the above-described process. Inkjet patterning (localized overoxidation) of the PEDOT:PSS nanofilm (Figure 1d) was performed just before the deposition of the PLA layer with a Dimatix Materials Printer DMP-2800 (Fujifilm Corp., Japan). The printhead cartridge used for inkjet was filled with an oxidating solution of sodium hypochlorite, NaClO (2 wt % solution in water) + 0.13 wt % Triton X-100. A thermal treatment on hot plate at T = 50 °C for 20 min was operated on the samples after the printing, followed by washing and rinsing with DI water and drying with nitrogen gun.

2.4. Nanosheets Surface and Electrical Characterization. The thickness of nanofilms and surface profile of the overoxidized patterns were characterized with a P-6 stylus profilometer (KLA Tencor, USA). The thickness t was measured by scratching the nanofilm with a needle and by measuring the height profile of the edge. Surface topography and roughness of the nanofilms were characterized by atomic force microscope (AFM) imaging, using a Veeco Innova scanning probe microscope. The images were collected operating in tapping mode, with oxide-sharpened silicon probes (RTESPA-CP) at a resonant frequency of ≈300 kHz. Measurements were performed in air, at room temperature, on samples collected and dried on a fresh silicon wafer after the release of the nanofilm from the supporting layer. Sample average roughness R_a in the AFM images were obtained by software analysis (Gwyddion SPM analysis tool).

Scanning electron microscope (SEM) images of the nanosheets collected on Si or on steel meshes were obtained with a Helios NanoLab 600i Dual Beam FIB/FE-SEM instrument (FEI, USA), operating at 5.0 kV accelerating voltage.

Electrical resistance R of the nanosheets was measured by using a homemade two-probe apparatus on square samples with lateral dimension of 1.5 cm. Conductivity σ has been calculated by making use of the following formulas: $R = \rho(l/A)$; $\sigma = 1/\rho$, where ρ is the resistivity of the nanosheet and l and $A = lt$ are, respectively, the length and the cross-sectional area of the sample.

2.5. Electrochemical Switching of Nanofilm Surface and Contact Angle Measurements. Electrochemical behavior of nanofilms has been investigated by cyclic voltammetry (CV) using a Reference 600 potentiostat/galvanostat (Gamry Instruments, Warminster, PA) in a three-electrode single-compartment cell containing a NaCl-water solution (0.1 M) as the electrolyte. PEDOT:PSS/PLA nanofilm sample acted as the working electrode (WE), a platinum wire as the counter electrode (CE), and Ag/AgCl as the reference electrode (RE). Measurements were performed on nanofilm samples suspended as a anchored nanomembrane on a Teflon ring (ext ⌀ = 10 mm, int ⌀ = 5 mm) onto which two gold electrodes have been sputtered for providing electrical contacts to the nanofilm; wires were connected with gold electrodes using silver paint and isolated with acrylic glue. The hole provided a sufficiently large area in which nanofilm was suspended.

CV experiments were carried out in the potential range from −1.0 to +1.0 V at different scan rates (v = 20, 50, 70, 100, 150, 200 mV/s). In the case of patterned nanofilms with interdigitated electrode geometry (IDE), that is, with two adjacent electrically isolated regions on the same nanosheet separated by an insulating gap, each side of the IDE was put in contact with a gold electrode and acted, respectively, as WE and CE, in order to obtain inverted polarity on separated electrodes.

For the electrochemical switching of the PEDOT:PSS surface, a 1 mM NaCl aqueous solution was used as the electrolyte; the nanosheet (with typical surface of 3 cm^2) was set as the WE, a platinum wire was

dx.doi.org/10.1021/am402142c | ACS Appl. Mater. Interfaces 2013, 5, 9461−9469

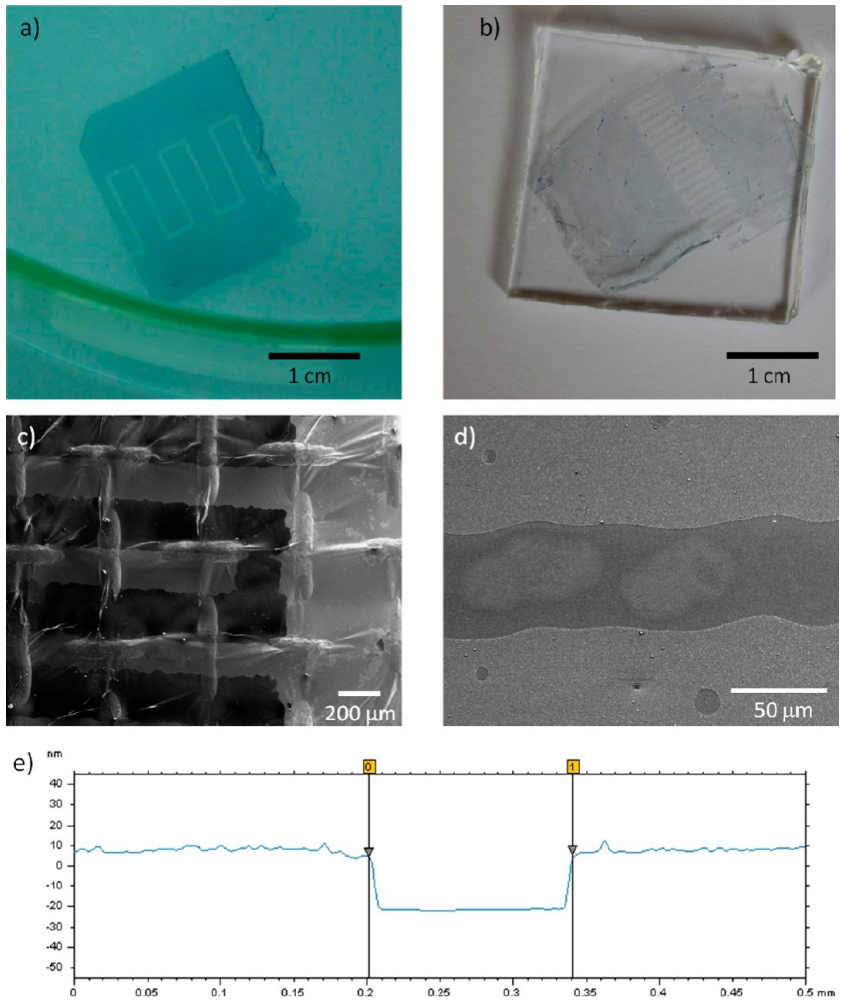

Figure 2. Inkjet patterned nanofilms. Pictures of nanofilms with interdigitated electrodes pattern: (a) free-standing, 1 mm gap size (floating in water); (b) collected on PDMS slab, 500 μm gap size. SEM images of (c) interdigitated electrodes pattern with 200 μm gap size (collected on a steel mesh) and (d) line pattern at the minimum attainable width, w_{act} = 50 μm. (e) Surface profile across an inkjet patterned line (100 μm width design).

used as the CE and set at a distance of 2 cm from WE, and the system was switched by using a 1.5 V AA battery (corresponding to a starting current density of ~30 μA/cm^2) for 30 s, that was the time needed for complete switching to the desired electrochemical state. As before, in the case of patterned nanosheets with IDE geometry, each side of the IDE was, respectively, connected to the positive or negative pole of the battery.

Contact angles were measured using the sessile drop method. Measurements were performed with a tensiometer Theta Lite (Attension) on the PEDOT:PSS side of the nanofilm collected on a clean polystyrene substrate, by dispensing 1 μL DI water droplets. The angle of contact was calculated via instrument software on optical images taken after 5 s since deposition. Calculated values were averaged among measurements taken at 10 different positions on at least three samples for each electrochemical state of the material: pristine, oxidized, and reduced.

Differential wetting on patterned nanofilms surfaces by water was visualized after the deposition of 10 μL DI drops. A digital microscope (Hirox, Japan) was used in order to capture side-view images of droplets deposited on the nanofilm surfaces and digital microscope software tools were used in order to measure the contact angle from captured images.

3. RESULTS AND DISCUSSION

3.1. Nanofilms Fabrication and Patterning. Based on a procedure that allows for fabricating single layer free-standing PEDOT:PSS nanofilms,[32] we further developed and optimized a process for obtaining patterned bilayer PEDOT:PSS/PLA nanofilms. The overall process of deposition, patterning, and release of nanofilms is schematized in Figure 1.

A thin PDMS layer on Si (Figure 1b) was used as the temporary substrate onto which to prepare and pattern the nanofilms. PDMS was selected due to the fact that a mild plasma treatment temporarily improves its surface hydrophilicity thus permitting the uniform deposition by spin coating of a PEDOT:PSS water dispersion. Due to its low glass transition temperature T_g and to the rearrangement of highly mobile polymer chains, PDMS surface exhibits a fast hydrophobic recovery at room temperature (typically in the order of some hours), and this effect is usually faced as an issue when permanent modification of the PDMS surface is needed, as in many applications.[34] On the contrary, in the case of our nanofilms, we turned this effect to our own advantage in order to recover PDMS hydrophobicity and repulsivity toward the PEDOT:PSS nanofilm, once the latter has been deposited and patterned. Thus, the nanofilm can be peeled off from the substrate with the aid of a thicker supporting film of PVA prepared by solution casting (Figure 1f–h).

Patterning of the conductive PEDOT:PSS layer was provided by means of a chemical overoxidation process with a sodium

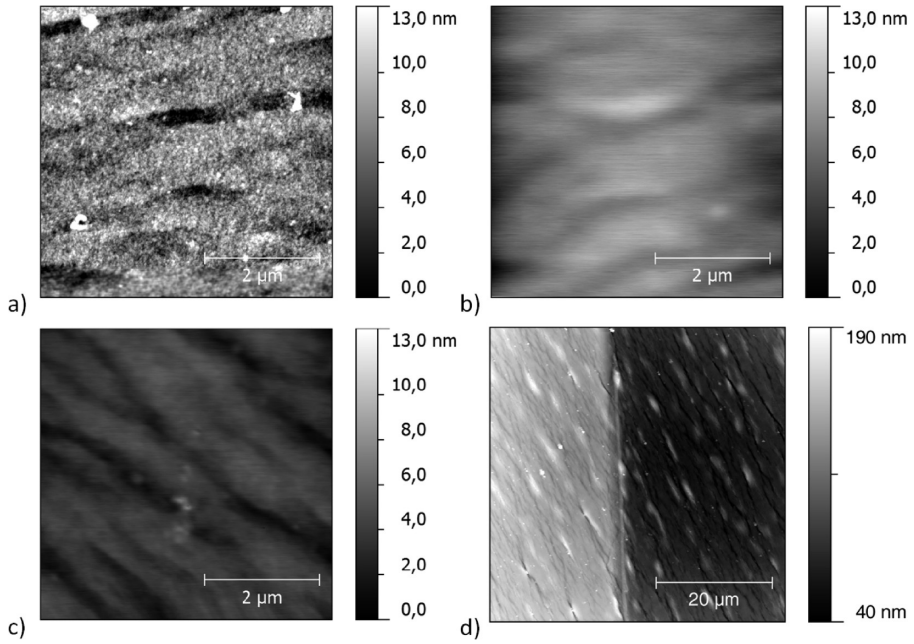

Figure 3. Surface topography of bilayer PLA/PEDOT:PSS patterned nanofilms as observed in AFM imaging. PEDOT:PSS side: (a) pristine PEDOT:PSS surface; (b) overoxidized surface. (c) PLA side; (d) pattern edge step (PEDOT:PSS, left; overoxidized PEDOT:PSS, right).

hypochlorite solution in water that is known to irreversibly break conjugation in polythiophenes (see inset chemical reaction scheme in Figure 1d), thus leading to suppression of electronic conductivity.[35] This subtractive chemical patterning approach has been tested in combination with various techniques, such as inkjet,[36] microcontact printing with agarose stamps soaked in deactivating solution,[37] silk screen printing, or also with photolithographically patterned resists.[38] Upon exposure of PEDOT or PEDOT:PSS to sodium hypochlorite, the process initially leads to deactivation only (with concomitant change in color from blue to transparent), while physical etching of the polymer results for longer times probably due to the simultaneous degradation of mechanical properties of the film that is mechanically removed in the following washing step.[37]

In this study, inkjet printing (Figure 1d) was chosen for patterning, since it provides a versatile, cheap, maskless and relatively fast noncontact process for patterning over large area nanofilms. Viscosity and wettability of the deactivating solution was properly set for the inkjet printing by adjusting the formulation of the "ink" that contained a 2 wt % solution in water of NaClO to which 0.13 wt % Triton X-100 surfactant was added. Additionally, moderate heating (T = 50 °C for 20 min) was provided to printed substrates in order to enhance the reaction of sodium hypochlorite. A final step of careful washing and rinsing with DI water was necessary in order to stop the reaction and to remove reactive salts crystallized on the surface after evaporation of the water contained in the ink. Various geometries of patterns were tested, such as straight lines, interdigitated electrodes (Figure 2a–d), or also rounded features, as in the case of the logo shown in Figure S1 (Supporting Information). In the bilayer nanofilm, with a total thickness $t = 258 \pm 13$ nm, a spin-coated PLA thin film acted as a passive layer providing mechanical robustness and continuity to the overall nanofilm structure. Indeed, the patterning process provided a complete etching of the ultrathin PEDOT:PSS layer (thickness $t \approx 45$ nm), as it was evidenced in profilometry and AFM measurements on PEDOT:PSS/PLA nanofilms collected on silicon after their release in water. In particular, Figure 2e shows the step profile of the nanofilm surface across the edge of an overoxidized line. An AFM image of pattern edge step is reported in Figure 3d. For these reasons we were not able to fabricate single layer PEDOT:PSS patterned nanofilms that could maintain integrity after the release. We selected PLA as a suitable support layer, because of its already tested behavior as a free-standing nanofilm[39−41] and for its good thermal and mechanical properties. Moreover its biocompatibility and longer-term biodegradability can impart interesting features to these nanofilms, envisioning applications in skin-contact devices or in other biomedical applications.[39−41]

Resolution and reproducibility of the printing process was assessed by SEM imaging and profilometry on samples with insulating lines printed at different nominal width w_{nom} (design width), that is, w_{nom} = 1000, 750, 500, 250, 100, and 50 μm. The actual width w_{act} of these printed lines was found to be larger, with difference almost constant in the overall range of study, $w_{act} - w_{nom} \sim 60$ μm. This is ascribable to lateral diffusion of deactivating solution on the plane. Given this finding, we corrected the drawing design of printing by taking into account this effect (i.e., by accordingly reducing the design line width): this was effective in reducing the difference between nominal and actual size of printed features. These results are reported in the Supporting Information. Width w_{act} = 50 μm was found to be the minimum attainable size for patterns (Figure 2d) because of the inherent spatial resolution of inkjet printing, that is limited to approximately 25 μm.

Nanofilm surface topography and roughness were characterized by AFM imaging at different locations on the patterned nanofilms (Figure 3), both on the PEDOT:PSS side and on the PLA side of the nanofilm. Pristine PEDOT:PSS surface (Figure 3a) showed the typical grain structure of this material, as already reported in the case of free-standing PEDOT:PSS nanofilms,[32] with average roughness R_a = 1.87 nm. The surface topography and roughness was quite different in printed

dx.doi.org/10.1021/am402142c | ACS Appl. Mater. Interfaces 2013, 5, 9461−9469

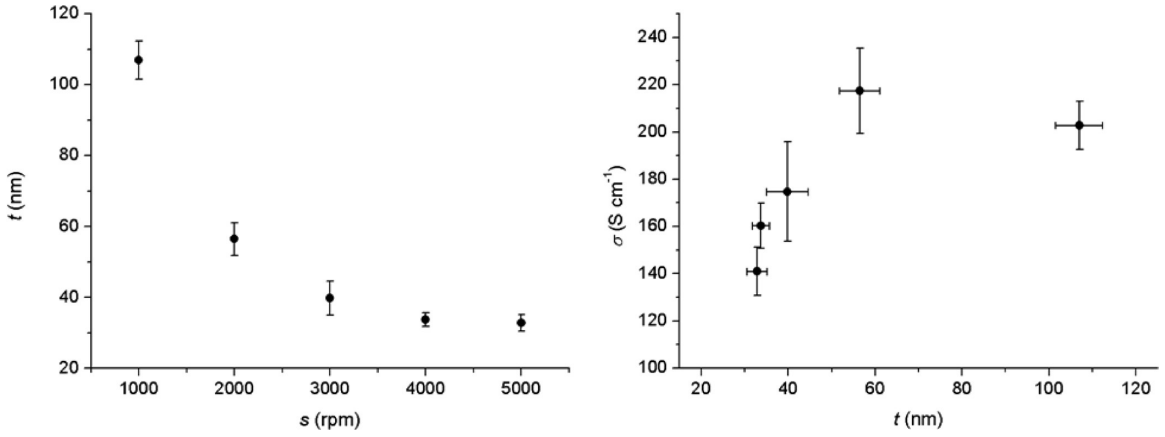

Figure 4. Thickness t of DMSO doped PEDOT:PSS layer as a function of fabrication parameters (spin-coating speed s) (left). Conductivity σ of DMSO doped PEDOT:PSS layer as a function of thickness t (right).

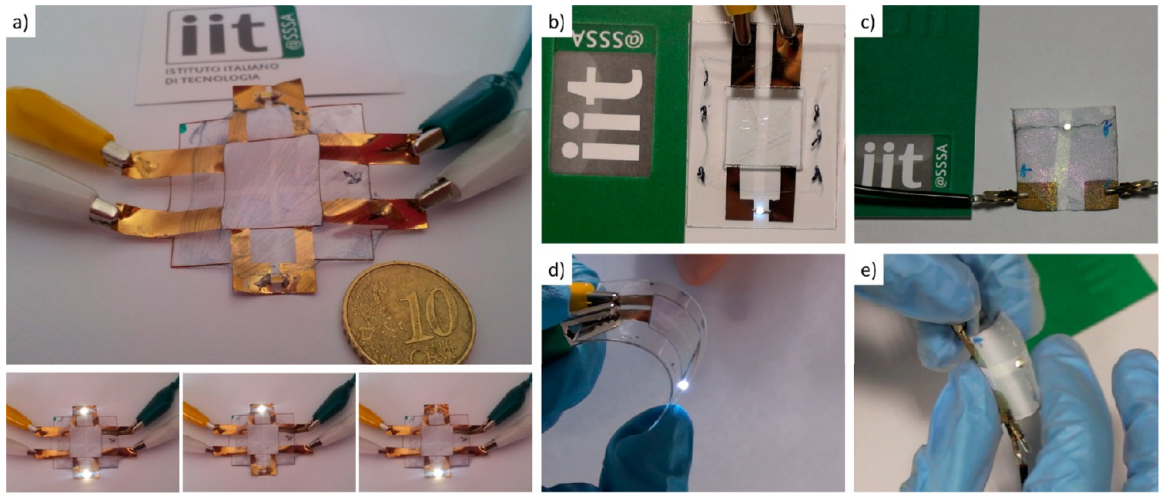

Figure 5. Simple demonstrators showing functioning of patterned nanofilms as conductors. a) Demonstrator 1: plastic frame with nanofilm suspended over a square hole and cross pattern separating nanofilm into 4 isolated electrodes allowing for independent switching of two LEDs; b) demonstrator 2: nanofilm suspended over the square hole of a plastic frame and patterned with two conducting lines connected to a LED, and d) its functioning while bending the frame; c) demonstrator 3: nanofilm collected on a piece of cotton fabric providing electrical contact to a LED glued on the fabric and e) its functioning while bending the fabric.

overoxidized lines (Figure 3b), with a roughness R_a = 1.14 nm and on the PLA side (Figure 3c), R_a = 0.7 nm. The thicker PLA layer showed microscale waviness (periodicity 1−2 μm), underlying the granular topography of PEDOT:PSS (Figure 3a), as already observed in the case of free-standing PLA nanofilms. The AFM image taken at the edge of a printed line (Figure 3d) clearly depicts the sharp step profile of the printed pattern.

3.2. Electrical Characterization. Addition to PEDOT:PSS of secondary dopants such as ethylene glycol, dimethyl sulfoxide, sorbitol or others in a typical range of 1−10 wt % content is known to greatly enhance the electronic conductivity of dried films.[42] To this aim, we added a 5 wt % of DMSO to the original PEDOT:PSS formulation. Conductivity of the nanofilms σ was evaluated by means of a two-probe resistance measurement on square samples with different thicknesses, as obtained by changing spin-coating speed in the PEDOT:PSS deposition step. Results of this characterization, along with the corresponding thickness of the PEDOT:PSS conductive layer as evaluated by stylus profilometry, are reported in Figure 4. Conductivity was slightly changing with thickness because of some percolation effects arising at low thickness, comparable with typical dimension of individual PEDOT-rich grains, as discussed and rationalized elsewhere.[32]

Typical conductivity of the nanofilms discussed hereinafter (thickness t = 45 nm) was around 180 S cm^{-1}, to be compared with σ = 1−10 S cm^{-1} for single layer PEDOT:PSS nanofilms without using DMSO as a secondary dopant agent.[32] This increase is totally in line with expectations and values reported in literature for films with similar materials composition deposited on bulk substrates.

3.3. Demonstrators of Suspended/Conformable Circuits Based on Bilayer Nanofilms. In order to demonstrate the functionality of the patterned conductive nanofilms in simple passive circuits, we built up some simple demonstrators in which nanofilms collected onto different substrates provided electrical contact for switching LED lights. These demonstrators were also intended to envision the application of nanofilms as ultrathin, floating, or conformable conductors.

In particular, we tested three different demonstrator configurations. Nanofilms were collected on flexible plastic frames as suspended nanomembranes over a square hole and their patterns allowed for switching of LEDs mounted on frames: demonstrator 1 (Figure 5a) had two LEDs that could

be independently switched on/off thanks to the cross pattern provided on the nanofilm (4 separated electrodes) and connecting to power supply; demonstrator 2 (Figure 5b,d) had one LED whose pins were connected to power supply through two separated conductive lines on the suspended nanofilm. Demonstrator 3 was realized by collecting a patterned nanofilm (two conducting pads separated by an insulating line) on a piece of cotton textile onto which a LED was previously attached. The nanofilm conformed to fabric and LED pins thus providing the necessary adhesion and electrical contact so that the LED can be switched on/off (Figure 5c,e). Movies of demonstrators 1−3 in operation under bending/rolling are provided in the Supporting Information.

3.4. Electrochemical Behavior. Besides their electronic conductivity, conducting polymers can also act as ionic conductors, and this two-fold functionality makes them attractive materials as transducers at the interface between electronic devices (electrons as charge carriers; operation in dry state) and the biological world (mostly based on ions as charge carriers; operation in water/fluids). Actually, up to date, CPs have been used in a number of devices (sensors, actuators, drug delivery systems, and cell scaffolds) which are based on this dual nature and exploit various interesting effects coming from electrochemical activation of these materials. Many properties of CPs, such as color, surface energy, protein adsorption, cell adhesion, and others, can be "switched" by applying a small voltage (0−1 V, typically), thus changing the redox state of the material. The change is often fully reversible. This smart behavior has been recently used for developing smart biointerfaces with differential (stem) cell adhesion,[43] electronic controlled detachment[44] or controlled release of ions,[45] and other organic bioelectronic devices.[21,29,43]

In order to investigate this switching on freely suspended nanofilms, we studied their electrochemical behavior in cyclic voltammetry (CV) experiments. CV of bilayer nanofilms recorded at different scan rates are reported in Figure 6. Typical reduction/oxidation peaks were observed, in line with similar findings obtained with supported PEDOT:PSS films. We simultaneously observed the change of color due to the electrochromic properties of PEDOT:PSS: dark blue for reduced state, to be compared with light blue/transparent for the oxidized state. This behavior has been confirmed in the case of patterned nanofilms with an interdigitated design (IDE) that were collected on a polytetrafluoroethylene (PTFE) ring frame as suspended nanomembranes. Wires and sputtered gold electrodes were provided on the frame for contacting each of two adjacent electrically isolated regions of IDE. One side was used as the working electrode and the other as the counter electrode during CV experiments. Alternate redox activation of different patterned areas on the same nanofilm was observed together with the corresponding electrochromic switching, as evidenced in insets of Figure 6.

3.5. Electrochemical Switching of Surface Properties: Angle of Contact. Based on the findings of CV experiments, we tested the surface energy of nanofilms and its modulation depending on the oxidation state of PEDOT:PSS by estimating the contact angle θ. Measurements were carried out both on suspended nanofilms ("free standing" nanofilms, collected over a plastic frame with a hole) and on nanofilms collected on bulk polystyrene sheets. First, we estimated contact angle θ on pristine (partially oxidized) PEDOT:PSS surface. Then, by shortly applying a small voltage while the nanofilm surface was immersed in an electrolytic solution, it was possible to

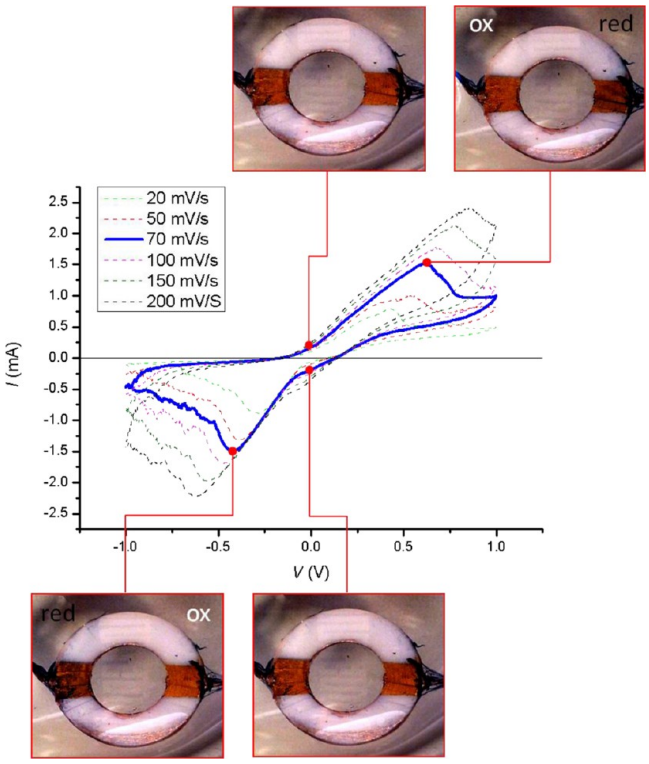

Figure 6. Electrochemical properties of patterned nanofilms suspended on plastic frame. The left side of interdigitated electrodes was set as the working electrode; the right side was set as the counter electrode. Cyclic voltammograms recorded at different scan rates in 0.1 M NaCl solution in water and corresponding pictures highlighting the electrochromic behavior of PEDOT:PSS.

electrochemically switch the surface. Reduction or oxidation could be obtained depending on the polarity of voltage that was addressed to the surface and the effect was fully reversible and repeatable, as also displayed as a change in color of the nanofilm. The results of these experiments are summarized in Figure 7. Lower contact angle θ was observed in the case of the reduced nanofilm surface, with respect to the oxidized (right) one, both for "free-standing" and supported nanofilms (Figure 7a). The effect was more pronounced in the latter case. Findings of these experiments on electronic control over the wettability are in good accordance with similar observations on PEDOT:tosylate films supported on polystyrene[26] that were rationalized on the basis of considerations about interaction of dipolar species and doping ions on the surface of the electrochemically active material, affecting the surface tension. Indeed, binding between the sulfonate ions (SO_3^- groups) of PSS and the PEDOT chains are strongly dependent on the electrochemical state of the latter. A lower surface energy (higher contact angle θ) is observed in the oxidized state, due to larger anchoring of polar SO_3^- groups to the PEDOT backbone. On the contrary, in the reduced state, such polar groups are exposed on the surface toward the water droplet, thus improving wettability. The ability to control wetting and adhesive properties of an electroactive polymer by means of electrochemical switching is currently explored also as a tool to control cell−surface interactions, such as to modulate and direct the attachment and proliferation of (stem) cells and/or to provide differentiative stimuli. The aim is to develop CP-based electroactive scaffolds for cell biology and tissue engineering, with many potential applications, for example, in

dx.doi.org/10.1021/am402142c | ACS Appl. Mater. Interfaces 2013, 5, 9461−9469

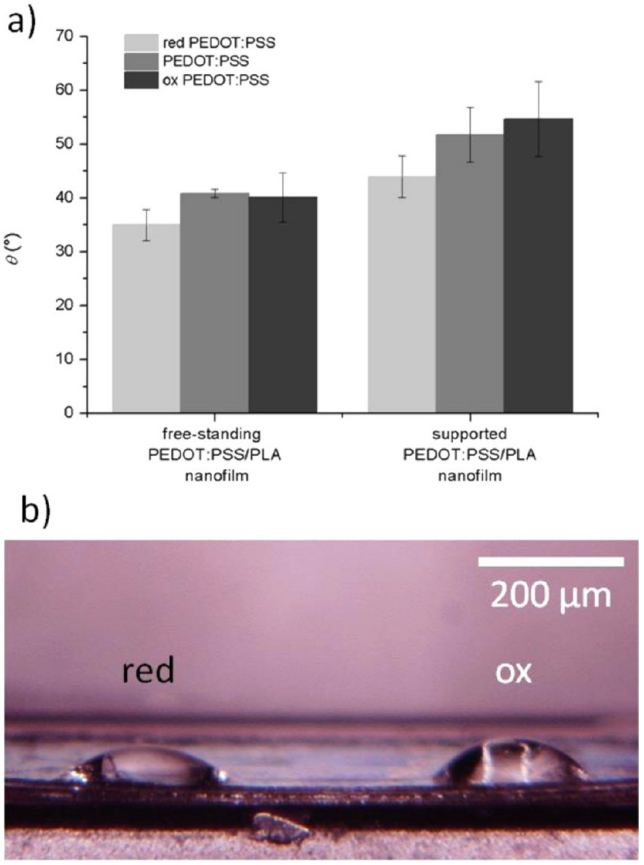

Figure 7. Electrochemical switching of wettability on PEDOT:PSS nanofilm surface. (a) Contact angle θ as measured at different red-ox states on free-standing nanofilm or nanofilm collected on polystyrene substrate. (b) Side-view microscope image of a free-standing PEDOT:PSS/PLA patterned nanofilm on which two water drops are placed on separated electrodes, switched to opposite redox states.

neuroprosthetics, bionics, and neural repair devices, among others. This approach has been explored in the case of neural cells[46] and stem cells,[26] epithelial cells,[27] or skeletal muscle cells;[28] interestingly, different cell types showed very different responses to same change in the oxidation state of CPs, and the results were correlated with surface wetting modification.[43] Recently, some studies provided useful insight in the mechanisms regulating these cell-surface interactions via protein adhesion and conformation change, tuned by electrical control of CP surface.[29,30]

In Figure 7b is reported a side-view microscope image of two water droplets deposited on the surface of a nanofilm that was patterned into two individually addressable electrode surfaces which were oppositely switched. Differential wetting is observed simultaneously on the same nanofilm, demonstrating the feasibility of localized surface switching that could be important for the use of our patterned nanofilms as smart biointerfaces.

4. CONCLUSION

Large area free-standing conductive nanofilms with patterned PEDOT:PSS were presented. Different microelectrodes geometries and patterns were fabricated with a subtractive patterning technique by means of an inkjet deposition of sodium hypochlorite. This permitted the localized over-oxidation of PEDOT:PSS causing the local irreversible loss of electrical conductivity, thus allowing the production of complex patterns with minimum size of individual lines around 50 μm. Thanks to their thickness, nanofilms showed ultrahigh conformability to complex surfaces and can be thus collected over several materials while retaining their functional properties, namely, electronic conductivity, electrochemical behavior, and switching of surface properties. The structure and properties of patterned bilayer PEDOT:PSS/PLA nanofilms were characterized, evidencing the different surface morphology of layers and patterned areas. Three simple demonstrators were built that permitted one to appreciate operation of the nanofilm as a conductor in air, that is, as a suspended nanomembrane or as a conductive skin over fabric, also during bending/rolling of the supporting material. The proposed nanofilms can find application as thin floating or ultraconformable circuits and (bio)electrical interfaces. Moreover, by taking advantage of PEDOT:PSS ionic conductivity and electrochemical behavior, nanofilms operation in an electrolyte solution was tested. Electrochemical switching of the surface with differential wettability upon redox activation of patterned nanofilms was assessed, permitting us to envision the application of these nanofilms as smart conductive biointerfaces for directing cell adhesion and differentiation.

■ ASSOCIATED CONTENT

Ⓢ Supporting Information

Two additional figures (Figures S1 and S2) and a video. Figure S1 shows pictures of different pattern design on nanofilms. Figure S2 contains two graphs with estimation of inkjet patterning quality and resolution. The video shows operation of the demonstrators 1−3 in which nanofilms acted as conductors in air. This material is available free of charge via the Internet at http://pubs.acs.org.

■ AUTHOR INFORMATION

Corresponding Author

*E-mail: francesco.greco@iit.it.

Notes

The authors declare no competing financial interest.

■ REFERENCES

(1) Someya, T.; Kato, Y.; Sekitani, T.; Iba, S.; Noguchi, Y.; Murase, Y.; Kawaguchi, H.; Sakurai, T. *Proc. Natl. Acad. Sci. U.S.A.* **2005**, *102*, 12321−12325.
(2) Rogers, J. A.; Huang, Y. *Proc. Natl. Acad. Sci. U.S.A.* **2009**, *106*, 10875−10876.
(3) Lacour, S. P.; Wagner, S.; Huang, Z.; Suo, Z. *Appl. Phys. Lett.* **2003**, *82*, 2404−2406.
(4) Graudejus, O.; Görrn, P.; Wagner, S. *ACS Appl. Mater. Interfaces* **2010**, *2*, 1927−1933.
(5) Moon, G. D.; Lim, G.-H.; Song, J. H.; Shin, M.; Yu, T.; Lim, B.; Jeong, U. *Adv. Mater.* **2013**, *25*, 2707−2712.
(6) Lipomi, D. J.; Lee, J. A.; Vosgueritchian, M.; Tee, B. C. K.; Bolander, J. A.; Bao, Z. *Chem. Mater.* **2011**, *24*, 373−382.
(7) Vosgueritchian, M.; Lipomi, D. J.; Bao, Z. *Adv. Funct. Mater.* **2012**, *22*, 421−428.
(8) Wagner, S.; Bauer, S. *MRS Bull.* **2012**, *37*, 207−213.
(9) Kim, D.-H.; Rogers, J. A. *Adv. Mater.* **2008**, *20*, 4887−4892.
(10) Rogers, J. A.; Someya, T.; Huang, Y. *Science* **2010**, *327*, 1603−1607.
(11) Kim, D. H.; Ahn, J. H.; Won, M. C.; Kim, H. S.; Kim, T. H.; Song, J.; Huang, Y. Y.; Liu, Z.; Lu, C.; Rogers, J. A. *Science* **2008**, *320*, 507−511.

(12) Kim, D. H.; Lu, N.; Ma, R.; Kim, Y. S.; Kim, R. H.; Wang, S.; Wu, J.; Won, S. M.; Tao, H.; Islam, A.; Yu, K. J.; Kim, T. I.; Chowdhury, R.; Ying, M.; Xu, L.; Li, M.; Chung, H. J.; Keum, H.; McCormick, M.; Liu, P.; Zhang, Y. W.; Omenetto, F. G.; Huang, Y.; Coleman, T.; Rogers, J. A. *Science* **2011**, *333*, 838−843.
(13) Kim, D.-H.; Viventi, J.; Amsden, J. J.; Xiao, J.; Vigeland, L.; Kim, Y.-S.; Blanco, J. A.; Panilaitis, B.; Frechette, E. S.; Contreras, D.; Kaplan, D. L.; Omenetto, F. G.; Huang, Y.; Hwang, K.-C.; Zakin, M. R.; Litt, B.; Rogers, J. A. *Nat. Mater.* **2010**, *9*, 511−517.
(14) Park, M.; Im, J.; Shin, M.; Min, Y.; Park, J.; Cho, H.; Park, S.; Shim, M.-B.; Jeon, S.; Chung, D.-Y.; Bae, J.; Park, J.; Jeong, U.; Kim, K. *Nat. Nanotechnol.* **2012**, *7*, 803−809.
(15) Khodagholy, D.; Doublet, T.; Gurfinkel, M.; Quilichini, P.; Ismailova, E.; Leleux, P.; Herve, T.; Sanaur, S.; Bernard, C.; Malliaras, G. G. *Adv. Mater.* **2011**, *23*, H268−H272.
(16) Sessolo, M.; Khodagholy, D.; Rivnay, J.; Maddalena, F.; Gleyzes, M.; Steidl, E.; Buisson, B.; Malliaras, G. G. *Adv. Mater.* **2013**, *25*, 2135−2139.
(17) Elschner, A.; Kirchmeyer, S.; Lovenich, W.; Merker, U.; Reuter, K. *PEDOT: principles and applications of an intrinsically conductive polymer*; CRC Press: Boca Raton, FL, 2010; pp 167−244.
(18) Brown, T. M.; Kim, J. S.; Friend, R. H.; Cacialli, F.; Daik, R.; Feast, W. J. *Appl. Phys. Lett.* **1999**, *75*, 1679−1681.
(19) Brown, T. M.; Cacialli, F. *J. Polym. Sci., Part B: Polym. Phys.* **2003**, *41*, 2649−2664.
(20) Nardes, A. M.; Kemerink, M.; de Kok, M. M.; Vinken, E.; Maturova, K.; Janssen, R. A. J. *Org. Electron.* **2008**, *9*, 727−734.
(21) Berggren, M.; Richter-Dahlfors, A. *Adv. Mater.* **2007**, *19*, 3201−3213.
(22) Malliaras, G. G. *Biochim. Biophys. Acta, Gen. Subj.* **2013**, *1830*, 4286−4287.
(23) Isaksson, J.; Kjall, P.; Nilsson, D.; Robinson, N. D.; Berggren, M.; Richter-Dahlfors, A. *Nat. Mater.* **2007**, *6*, 673−9.
(24) Simon, D. T.; Kurup, S.; Larsson, K. C.; Hori, R.; Tybrandt, K.; Goiny, M.; Jager, E. W.; Berggren, M.; Canlon, B.; Richter-Dahlfors, A. *Nat. Mater.* **2009**, *8*, 742−6.
(25) Lin, P.; Yan, F. *Adv. Mater.* **2012**, *24*, 34−51.
(26) Saltó, C.; Saindon, E.; Bolin, M.; Kanciurzewska, A.; Fahlman, M.; Jager, E. W. H.; Tengvall, P.; Arenas, E.; Berggren, M. *Langmuir* **2008**, *24*, 14133−14138.
(27) Svennersten, K.; Bolin, M. H.; Jager, E. W. H.; Berggren, M.; Richter-Dahlfors, A. *Biomaterials* **2009**, *30*, 6257−6264.
(28) Greco, F.; Fujie, T.; Ricotti, L.; Taccola, S.; Mazzolai, B.; Mattoli, V. *ACS Appl. Mater. Interfaces* **2013**, *5*, 573−584.
(29) Wan, A. M. D.; Schur, R. M.; Ober, C. K.; Fischbach, C.; Gourdon, D.; Malliaras, G. G. *Adv. Mater.* **2012**, *24*, 2501−2505.
(30) Gelmi, A.; Higgins, M. J.; Wallace, G. G. *Small* **2013**, *9*, 393−401.
(31) Higgins, M. J.; Molino, P. J.; Yue, Z.; Wallace, G. G. *Chem. Mater.* **2012**, *24*, 828−839.
(32) Greco, F.; Zucca, A.; Taccola, S.; Menciassi, A.; Fujie, T.; Haniuda, H.; Takeoka, S.; Dario, P.; Mattoli, V. *Soft Matter* **2011**, *7*, 10642−10650.
(33) Greco, F.; Zucca, A.; Taccola, S.; Menciassi, A.; Dario, P.; Mattoli, V. *MRS Online Proc. Libr.* **2012**, *1403*, 253−258.
(34) Zhou, J.; Ellis, A. V.; Voelcker, N. H. *Electrophoresis* **2010**, *31*, 2−16.
(35) Yoshioka, Y.; Jabbour, G. E. In *Conjugated Polymers: Processing and Applications*, 3rd ed.; Skotheim, T. A. R., John, R., Eds.; CRC Press: Boca Raton, FL, 2007; pp 3-1−3-21.
(36) Yoshioka, Y.; Calvert, P. D.; Jabbour, G. E. *Macromol. Rapid Commun.* **2005**, *26*, 238−246.
(37) Hansen, T. S.; West, K.; Hassager, O.; Larsen, N. B. *Adv. Mater.* **2007**, *19*, 3261−3265.
(38) Tehrani, P.; Robinson, N., D.; Kugler, T.; Remonen, T.; Hennerdal, L.-O.; Häll, J.; Malmström, A.; Leenders, L.; Berggren, M. *Smart Mater. Struct.* **2005**, *14*, N21.
(39) Okamura, Y.; Kabata, K.; Kinoshita, M.; Saitoh, D.; Takeoka, S. *Adv. Mater.* **2009**, *21*, 4388−4392.
(40) Ricotti, L.; Taccola, S.; Pensabene, V.; Mattoli, V.; Fujie, T.; Takeoka, S.; Menciassi, A.; Dario, P. *Biomed. Microdevices* **2010**, *12*, 809−819.
(41) Pensabene, V.; Taccola, S.; Ricotti, L.; Ciofani, G.; Menciassi, A.; Perut, F.; Salerno, M.; Dario, P.; Baldini, N. *Acta Biomater.* **2011**, *7*, 2883−2891.
(42) Elschner, A.; Kirchmeyer, S.; Lovenich, W.; Merker, U.; Reuter, K. *PEDOT: principles and applications of an intrinsically conductive polymer*; CRC Press: Boca Raton, FL, 2010; pp 149−156.
(43) Svennersten, K.; Larsson, K. C.; Berggren, M.; Richter-Dahlfors, A. *Biochim. Biophys. Acta, Gen. Subj.* **2011**, *1810*, 276−285.
(44) Persson, K. M.; Karlsson, R.; Svennersten, K.; Löffler, S.; Jager, E. W. H.; Richter-Dahlfors, A.; Konradsson, P.; Berggren, M. *Adv. Mater.* **2011**, *23*, 4403−4408.
(45) Isaksson, J.; Kjäll, P.; Nilsson, D.; Robinson, N.; Berggren, M.; Richter-Dahlfors, A. *Nat. Mater.* **2007**, *6*, 673−679.
(46) Collazos-Castro, J. E.; Polo, J. L.; Hernández-Labrado, G. R.; Padial-Cañete, V.; García-Rama, C. *Biomaterials* **2010**, *31*, 9244−55.